

Ligand Effects on Cooperative Supramolecular Polymerization of Platinum(II) Acetylide Complexes

Zhao Gao, Junlong Zhu, Yifei Han, Xiaoqin Lv, Xiaolong Zhang, and Feng Wang*

*CAS Key Laboratory of Soft Matter Chemistry,
iChEM (Collaborative Innovation Center of Chemistry for Energy Materials),
Department of Polymer Science and Engineering,
University of Science and Technology of China,
Hefei, Anhui 230026 (P. R. China)
E-mail: drfwang@ustc.edu.cn*

Supporting Information

1.	<i>Materials and methods</i>	S2
2.	<i>Synthetic routes to the targeted monomers 1–3</i>	S3
3.	<i>UV/Vis measurements of 1–3 in chloroform solution</i>	S12
4.	<i>Concentration-dependent UV/Vis measurements of 2–3</i>	S12
5.	<i>UV/Vis measurements of 2–3 in different solvents</i>	S13
6.	<i>CD cooling curves of 1–2</i>	S14
7.	<i>¹H NMR dilution experiments for 1–3</i>	S14
8.	<i>Fluorescent measurements of 1–3</i>	S16

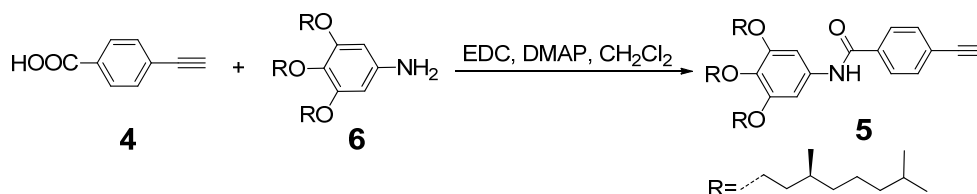
1. Materials and methods

Methyl 4-ethynyl benzoate, pyrogallol, 4-dimethylamino pyridine (DMAP), *N*-(3-dimethylaminopropyl)-*N'*-ethylcarbodiimide hydrochloride (EDC•HCl), *trans*-PtCl₂(PR'₃)₂ (R' = Me, Et, and Bn) are reagent grade and used as received. Compound **6** was synthesized according to the previously reported procedure.^{S1} Spectrophotometric grade methylcyclohexane and chloroform are purchased from Adamas Reagent, Ltd.

¹H NMR spectra were collected on a Varian Unity INOVA-300 spectrometer with TMS as the internal standard. ¹³C NMR spectra were recorded on a Varian Unity INOVA-300 spectrometer at 75 MHz. MALDI-TOF experiments were recorded on a Bruker Autoflex Speed spectrometer using DCTB as the matrix. UV/Vis spectra were recorded on a UV-1800 Shimadzu spectrometer. Circular dichroism (CD) measurements were performed on a Jasco J-1500 dichrograph equipped with a PFD-425S/15 Peltier-type temperature controller. Solution excitation and steady-state fluorescence emission spectra were recorded on a FluoroMax-4 spectrofluorometer (Horiba Scientific) and analyzed with an Origin (v8.0) integrated software FluoroEssence (v2.2). Transmission electron microscope (TEM) images from samples in solution were performed on a Tecnai G2 Spirit BioTWIN electron microscope, operating at an acceleration voltage of 120 kV. For the observation of aggregates, a drop of sample solution (5×10^{-4} M) was placed on a copper grid and air-dried. Rheological characterization was performed by using a TA ARG2 stress-controlled rheometer with 40 mm parallel plates geometry. Gel of the compound was transferred onto the plate kept at 283 K. In order to avoid the solvent evaporation, the surface of sample between two plates was covered with glycerol. Oscillatory dynamic shear experiments were performed in the frequency range of 0.1-300 rad/s, using a constant strain (0.2%) determined with a strain sweep to lie within the linear viscoelastic regime. The evolution of moduli (G' and G'') vs time was tested at 283 K, with a frequency of 1 Hz and a strain of 0.2%.

2. Synthetic routes to the targeted monomers 1–3

2.1. Synthesis of compound 5



Compounds **4** (71.5 mg, 0.49 mmol) and **6** (250 mg, 0.45 mmol) were dissolved in CH_2Cl_2 (6 mL). EDC·HCl (171 mg, 0.89 mmol) and DMAP (10.9 mg, 0.089 mmol) were added and stirred at room temperature for 24 hours. The solution was extracted with $\text{H}_2\text{O}/\text{CH}_2\text{Cl}_2$ for three times. The organic extracts were then combined and concentrated under reduced pressure to afford a yellow oil, which was subjected to flash column chromatography (silica gel, petroleum ether/ CH_2Cl_2 , 5 : 1 v/v as the eluent) to provide **5** as a yellow oil (246 mg, 80%).^{S1} ^1H NMR (300 MHz, CDCl_3) δ (ppm): 7.81 (d, $J = 8.3$ Hz, 2H), 7.72 (s, 1H), 7.59 (d, $J = 8.3$ Hz, 2H), 6.91 (s, 2H), 3.99 (m, 6H), 3.23 (s, 1H), 1.84 (m, 3H), 1.69 (d, $J = 4.6$ Hz, 4H), 1.58–1.44 (m, 5H), 1.33 (d, $J = 6.5$ Hz, 12H), 1.15 (m, 10H), 0.93 (d, $J = 6.4$ Hz, 9H), 0.86 (d, $J = 6.6$ Hz, 18H).

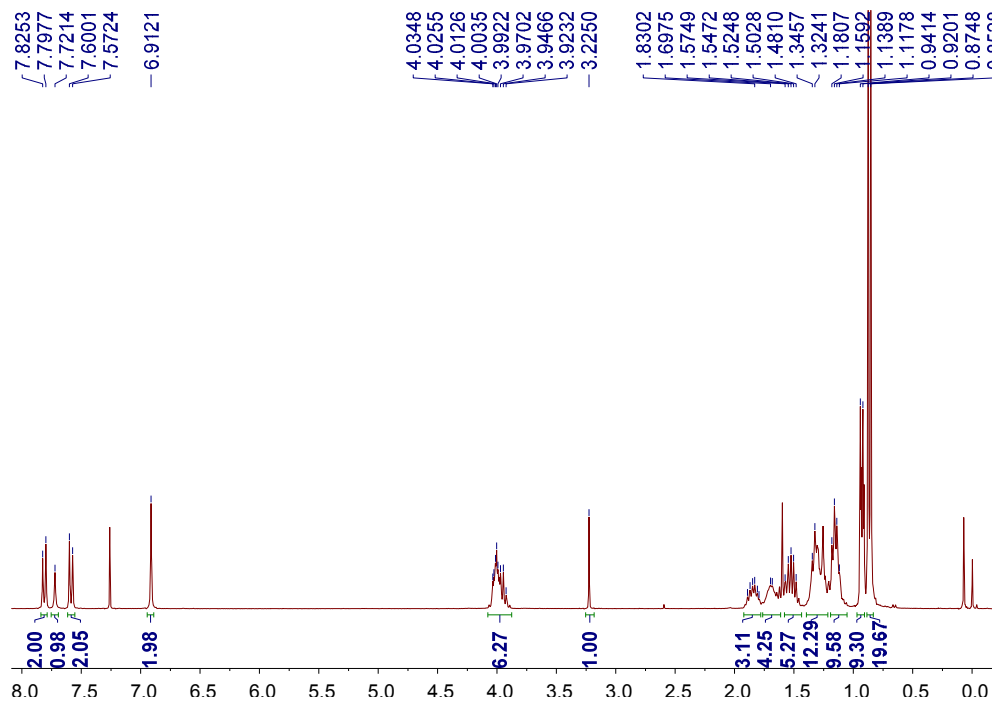


Figure S1. ^1H NMR spectrum (300 MHz, CDCl_3 , room temperature) of compound **5**.

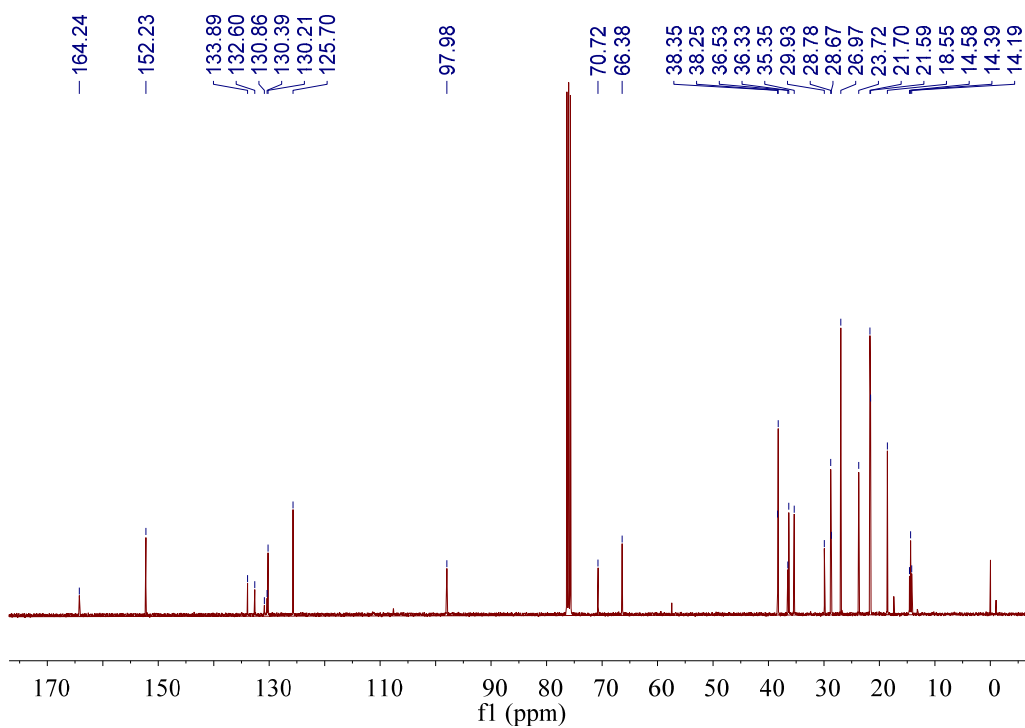


Figure S3. ^{13}C NMR spectrum (75 MHz, CDCl_3 , room temperature) of compound **1**.

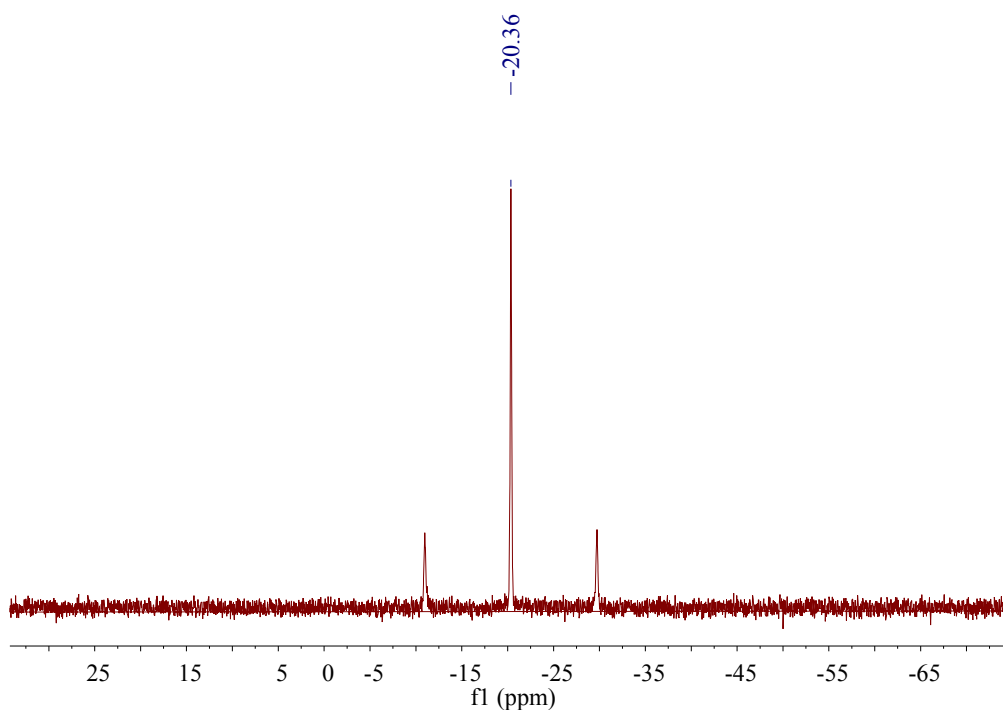


Figure S4. ^{31}P NMR spectrum (121.5 MHz, CDCl_3 , room temperature) of compound **1**.

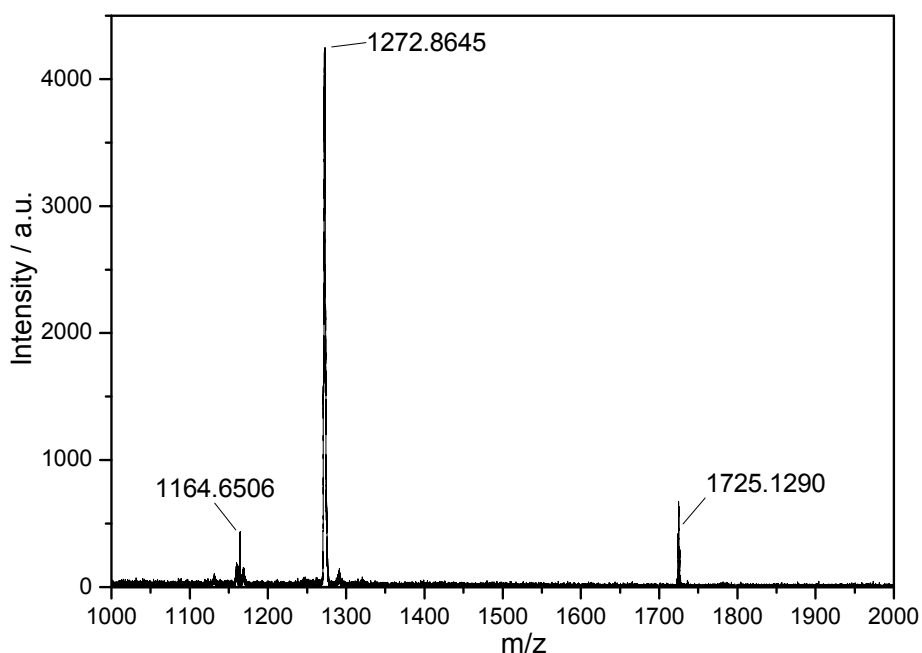
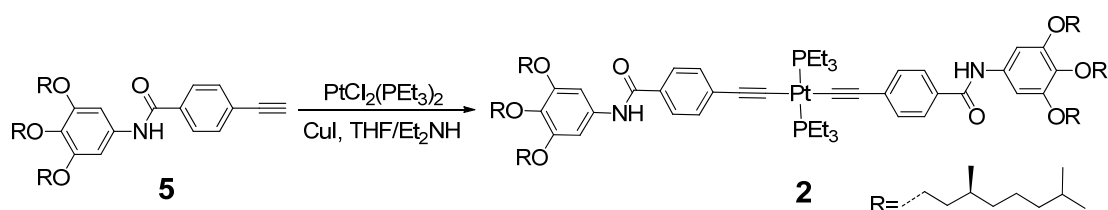


Figure S5. MALDI-TOF mass spectrum of compound **1**.

2.4. Synthesis of monomer **2**



Compound **5** (250 mg, 0.36 mmol), *trans*-PtCl₂(PEt₃)₂ (113 mg, 0.17 mmol), CuI (6.30 mg, 0.03 mmol) were mixed in THF/Et₂NH (9 mL, 2 : 1, *v/v*) and stirred at room temperature for 48 hours. The solvent was evaporated and the resulting mixture was extracted between water and CH₂Cl₂. The combined organic layer was dried over anhydrous Na₂SO₄, filtered and the solvent removed with a rotary evaporator to give a deep-yellow solid, which was subjected to flash column chromatography (silica, CH₂Cl₂ as the eluent) to afford **2** as pale yellow solid (265 mg, 89%). ¹H NMR (300 MHz, CDCl₃) δ (ppm): 7.72 (d, *J* = 8.3 Hz, 4H), 7.66 (s, 2H), 7.35 (d, *J* = 8.0 Hz, 4H), 6.92 (s, 4H), 4.08–3.88 (m, 12H), 2.24–2.13 (m, 12H), 1.84 (m, 6H), 1.70 (m, 6H), 1.61–1.46 (m, 12H), 1.38–1.28 (m, 16H), 1.28–1.19 (m, 24H), 1.15 (m, 20H), 0.97–0.90 (m, 18H), 0.87 (d, *J* = 6.6 Hz, 36H). ¹³C NMR (75 MHz, CDCl₃) δ (ppm): 164.27, 152.26, 133.95, 132.64, 131.65, 130.09, 130.00, 125.68, 98.01, 70.74, 66.43, 38.36, 38.27, 36.54, 36.35, 36.32, 35.38, 28.80, 28.69, 26.98, 23.72, 21.70, 21.59, 18.57, 15.65, 15.41, 7.36. ³¹P NMR (121.5 MHz, CDCl₃, room temperature) δ (ppm):

11.25 (s, ^{195}Pt satellites, $^1J_{\text{Pt-P}} = 1177.7$ Hz). MALDI-TOF-MS m/z : $[\text{M}+\text{H}]^+$, $\text{C}_{102}\text{H}_{171}\text{N}_2\text{O}_8\text{P}_2\text{Pt}$, calculated 1809.2150; found 1809.2162.

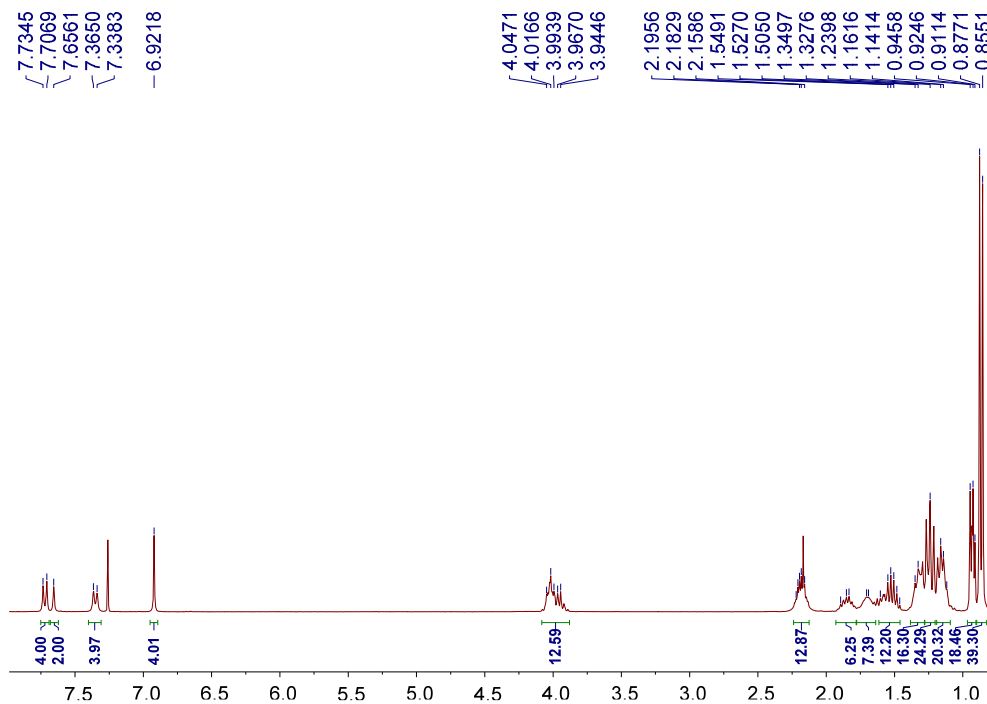


Figure S6. ^1H NMR spectrum (300 MHz, CDCl_3 , room temperature) of compound **2**.

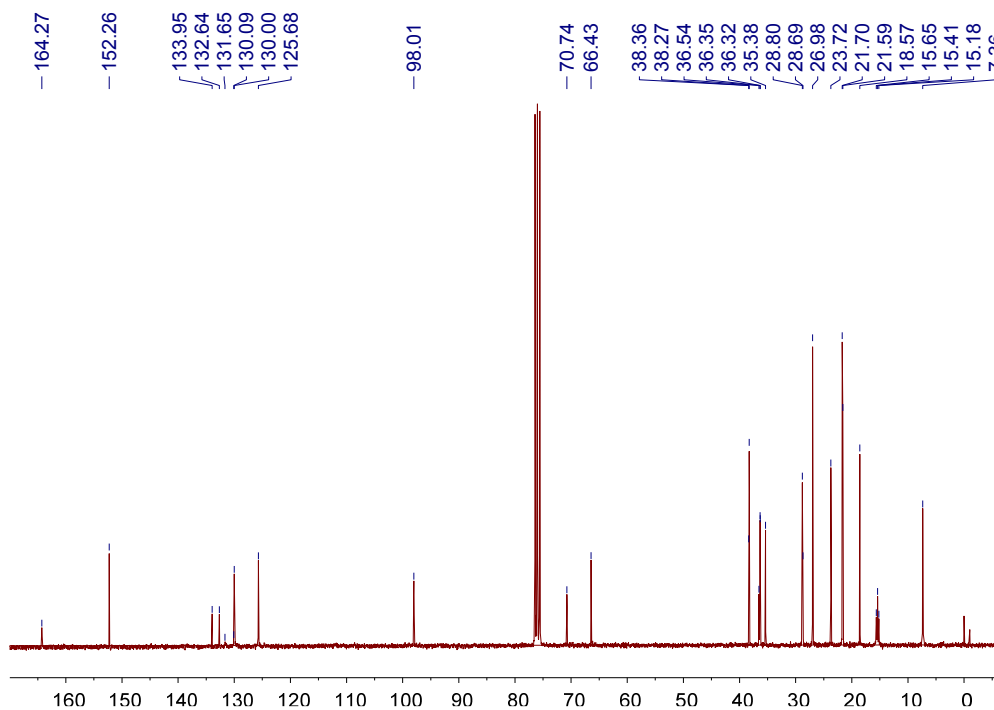


Figure S7. ^{13}C NMR spectrum (75 MHz, CDCl_3 , room temperature) of compound **2**.

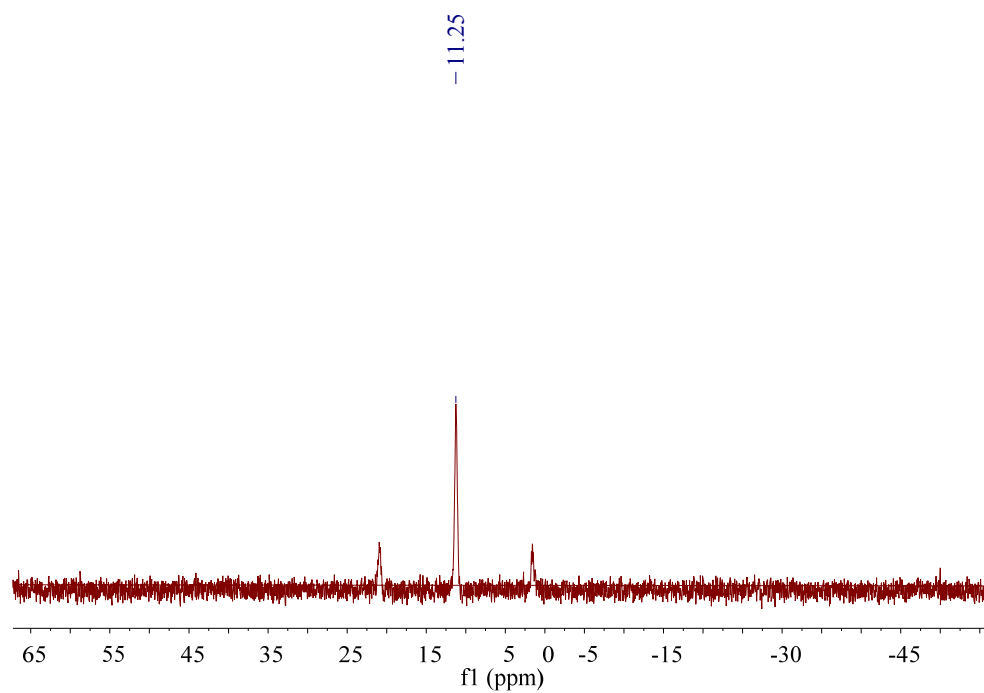


Figure S8. ^{31}P NMR spectrum (121.5 MHz, CDCl_3 , room temperature) of compound **2**.

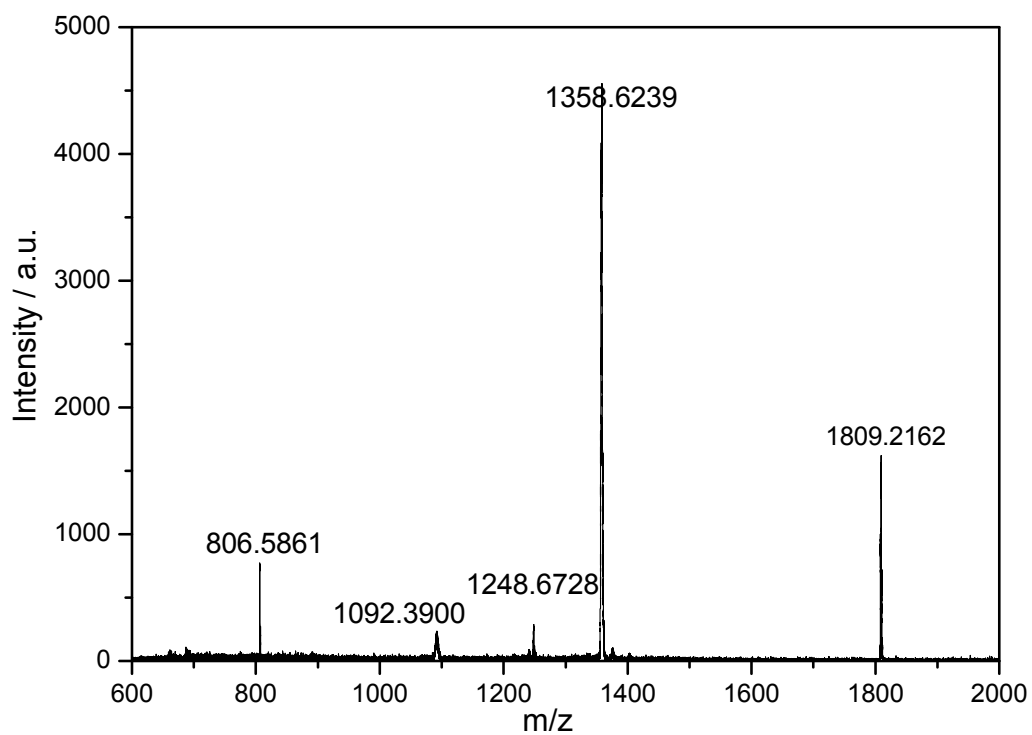
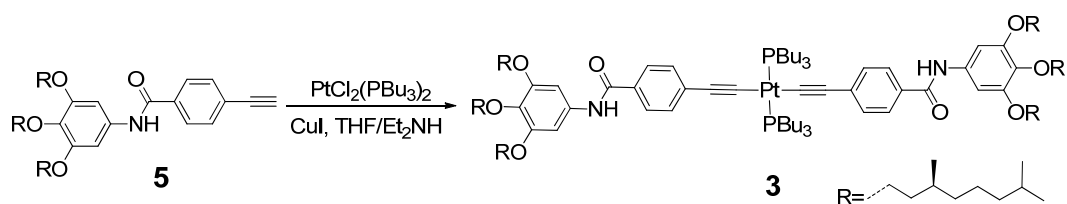


Figure S9. MALDI-TOF mass spectrum of compound **2**.

2.5. Synthesis of monomer **3**



Compound **5** (200 mg, 0.29 mmol), *trans*-PtCl₂(PBu₃)₂ (120 mg, 0.14 mmol), CuI (5.30 mg, 0.03 mmol) were mixed in THF/Et₂NH (9 mL, 2 : 1, v/v), and stirred at room temperature for 48 hours. The solvent was evaporated and the resulting mixture was extracted between water and CH₂Cl₂. The combined organic layer was dried over anhydrous Na₂SO₄, filtered and the solvent removed with a rotary evaporator to give a deep-yellow solid, which was subjected to flash column chromatography (CH₂Cl₂ as the eluent) to afford **3** as pale yellow solid (207 mg, 74%). ¹H NMR (300 MHz, CDCl₃) δ (ppm): 7.71 (d, *J* = 8.2 Hz, 4H), 7.64 (s, 2H), 7.33 (d, *J* = 8.0 Hz, 4H), 6.92 (s, 4H), 4.07–3.92 (m, 12H), 2.20–2.07 (m, 12H), 1.85 (m, 6H), 1.68–1.54 (m, 20H), 1.54–1.40 (m, 20H), 1.31 (m, 28H), 1.18 (m, 20H), 0.94 (m, 36H), 0.87 (d, *J* = 6.6 Hz, 36H). ¹³C NMR (75 MHz, CDCl₃) δ (ppm): 164.32, 152.26, 133.94, 132.65, 131.80, 129.87, 129.70, 125.63, 98.03, 70.73, 66.43, 38.36, 38.27, 36.53, 36.34, 35.37, 28.69, 26.98, 25.35, 23.72, 23.39, 22.98, 22.75, 21.70, 21.59, 18.57, 12.79. ³¹P NMR (121.5 MHz, CDCl₃, room temperature) δ (ppm): 3.37 (s, ¹⁹⁵Pt satellites, ¹*J*_{Pt-P} = 1163.7 Hz). MALDI-TOF-MS *m/z*: [M+H]⁺, C₁₁₄H₁₉₅N₂O₈P₂Pt, calculated 1977.4036; found 1977.4193.

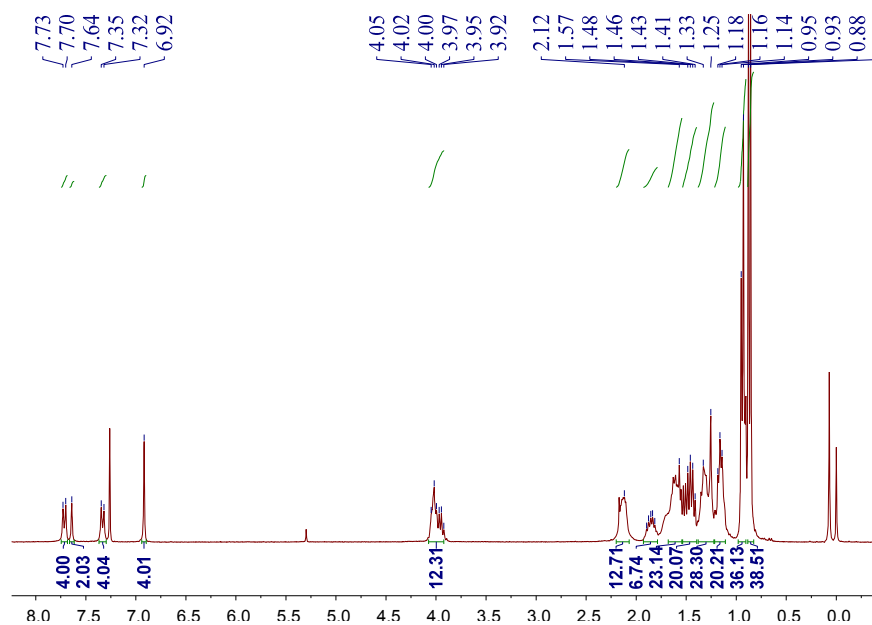


Figure S10. ¹H NMR spectrum (300 MHz, CDCl₃, room temperature) of **3**.

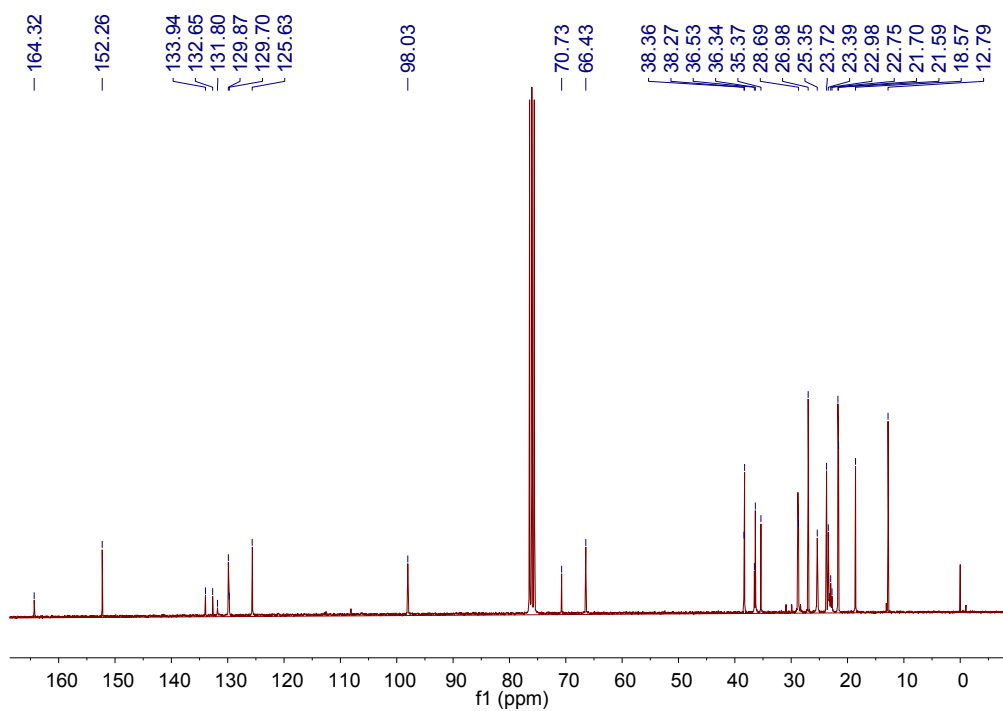


Figure S11. ^{13}C NMR spectrum (75 MHz, CDCl_3 , room temperature) of **3**.

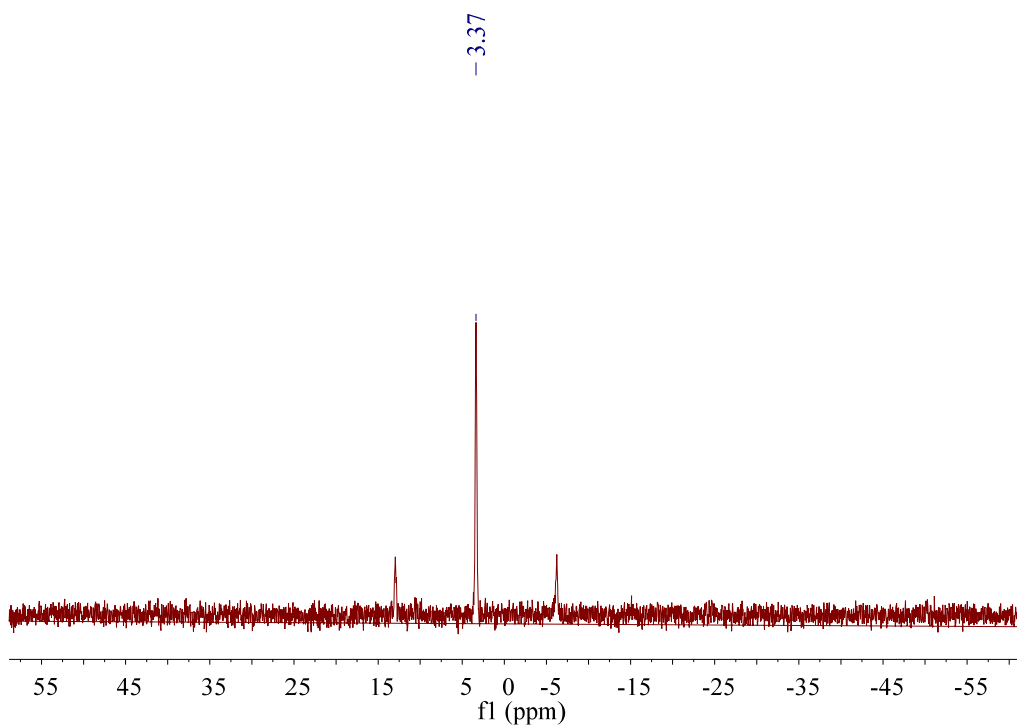


Figure S12. ^{31}P NMR spectrum (121.5 MHz, CDCl_3 , room temperature) of **3**.

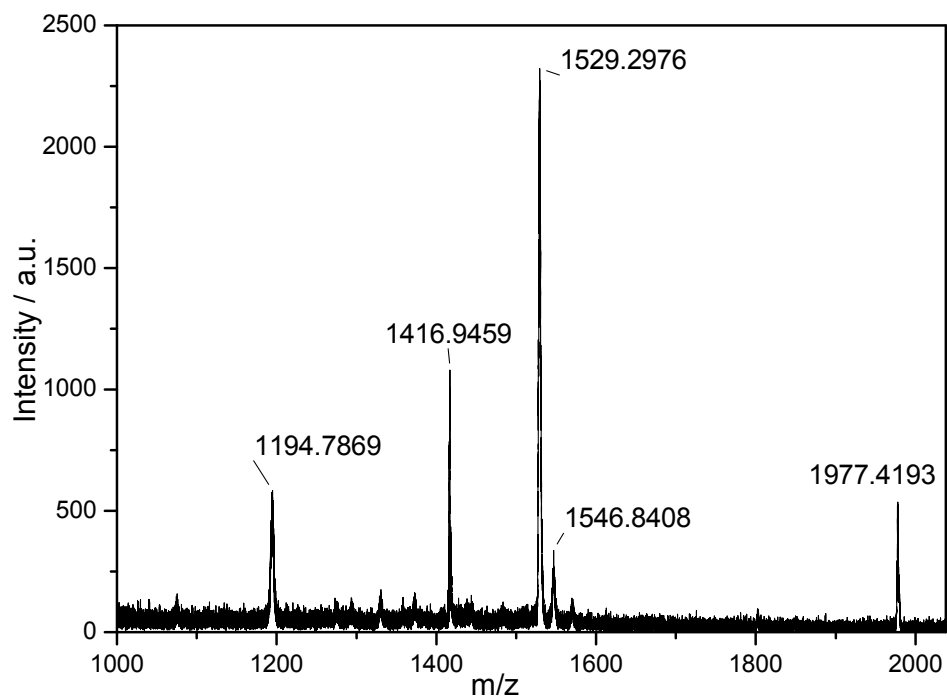


Figure S13. MALDI-TOF mass spectrum of **3**.

3. UV/Vis measurements of 1–3 in chloroform solution

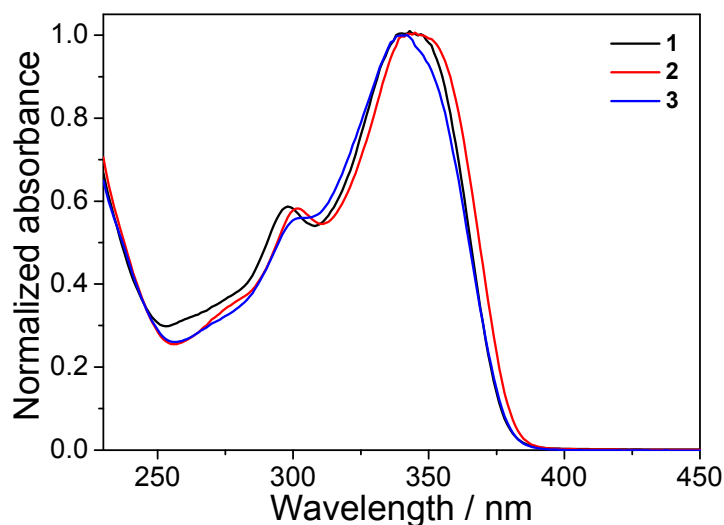


Figure S14. UV-Vis absorption spectra of **1–3** (2×10^{-4} M in chloroform). Similar spectral profiles are observed for **1–3**, suggesting that different alkyl substitutes on the PR'_3 ligands exert minor effects on the UV-Vis absorption signals of the platinum(II) acetylide complexes.

4. Concentration-dependent UV/Vis measurements of 2–3

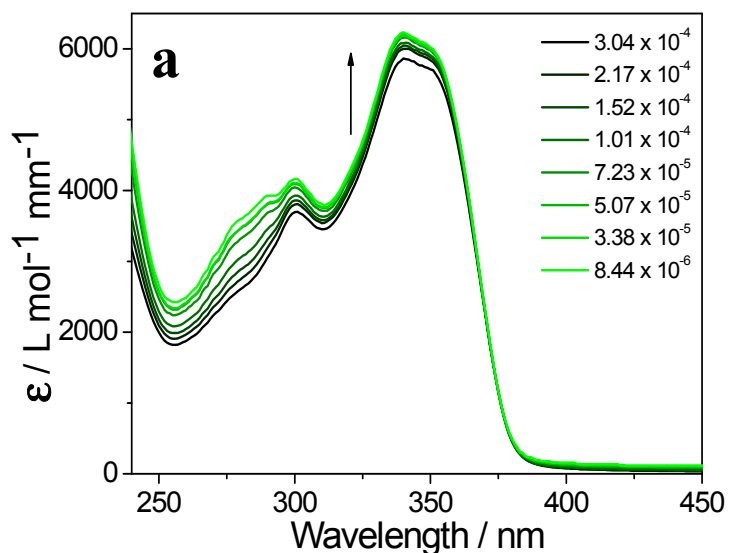


Figure S15. Concentration-dependent UV/Vis spectra of **2** in MCH/ CHCl_3 (99 : 1, v/v). No obvious isobestic points can be observed for **2**, which are distinct from those of **1**. Such results suggest that no transition between molecularly dissolved and aggregated states occurs for **2** under the experimental conditions.

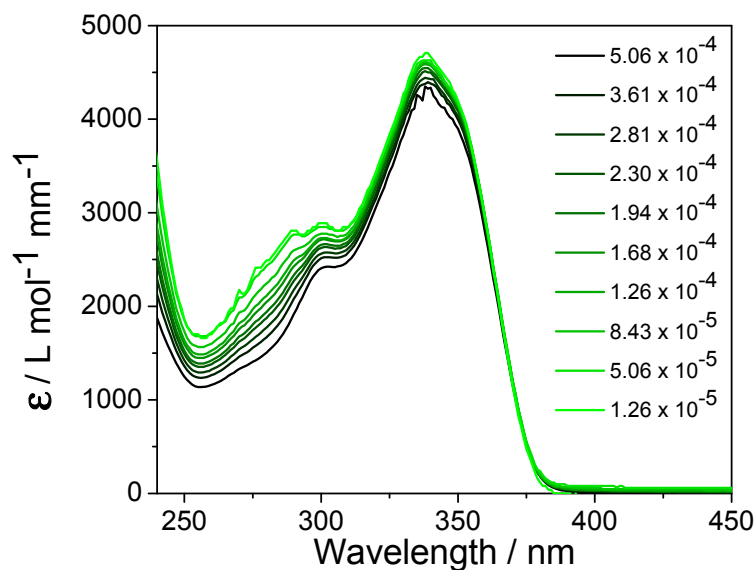


Figure S16. Concentration-dependent UV/Vis spectra of **3** in MCH/CHCl₃ (99 : 1, v/v). No isobestic points can be observed for **3**, which are distinct from those of **1**. Such results suggest that no transition between molecularly dissolved and aggregated states occurs for **3** under the experimental conditions.

5. UV/Vis measurements of **2–3** in different solvents

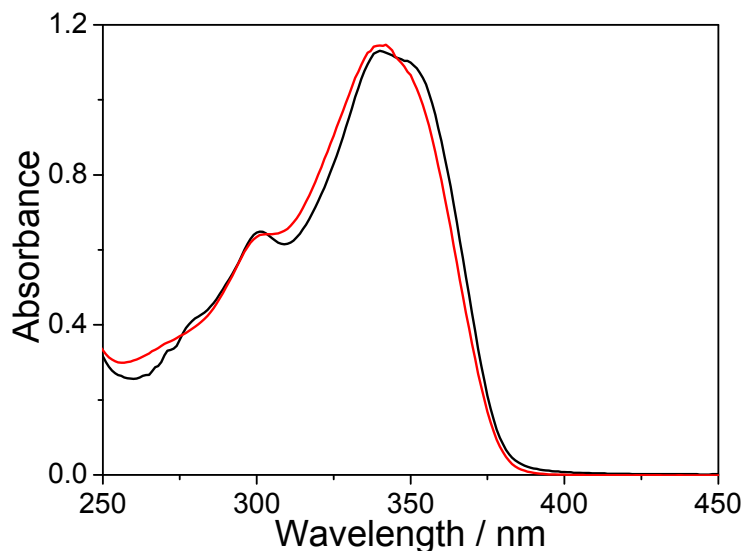


Figure S17. UV/Vis spectra of **2** (0.20 mM) in CHCl₃ (red line) and MCH/CHCl₃ (99 : 1, v/v) (black line). **2** exhibits slight absorption change when changing the solvents ($\lambda_{\text{max}} = 340$ nm in CHCl₃, versus $\lambda_{\text{max}} = 340$ nm with a shoulder peak at 350 nm in MCH/CHCl₃ (99 : 1, v/v)).

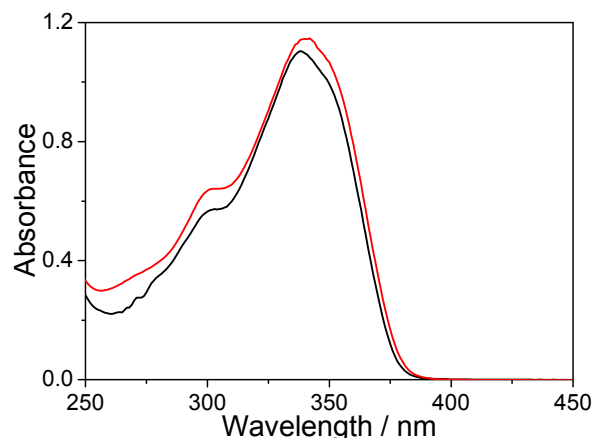


Figure S18. UV/Vis spectra of **3** (0.20 mM) in CHCl_3 (red line) and MCH/CHCl_3 (99 : 1, v/v) (black line). **3** exhibits slight absorption change when changing the solvents ($\lambda_{\text{max}} = 340$ nm in CHCl_3 , versus $\lambda_{\text{max}} = 339$ nm in MCH/CHCl_3 (99 : 1, v/v)).

6. CD cooling curves of 1–2

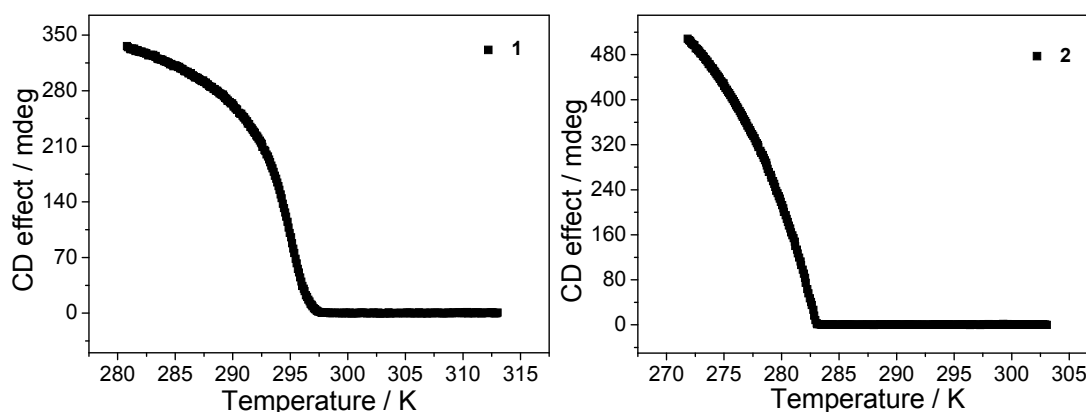


Figure S19. CD signals ($\lambda = 370$ nm) as a function of temperature for **1** (left) and **2** (right) (0.20 mM for both monomers) in MCH/CHCl_3 (99 : 1, v/v).

7. ^1H NMR dilution experiments for 1–3

Besides **1**, ^1H NMR dilution experiments were also performed for **2** and **3** (from 30.0 mM to 0.30 mM for each monomer, Fig. S20–S21). As can be seen, the chemical resonances of NH show gradual upfield shifts upon dilution, indicating that the monomers are prone to associate with each other at high monomer concentration. The representative plots of the proton resonance versus concentration are shown in Figure 3b. For a fast exchanging system, the observed chemical shift is the weighted average of the chemical shifts for the two exchanging species, as given by Eq. S3:^{S2}

$$\bar{\delta}_{\text{obs}} = \bar{\delta}_{\text{m}} + (\bar{\delta}_{\text{c}} - \bar{\delta}_{\text{m}}) f_{\text{c}} \quad \text{Eq. (S3)}$$

In particular, δ_{obs} , δ_{m} , and δ_{c} are the observed, monomeric (at infinite diluted state) and co-assembled (at infinite concentrated state) chemical shifts, respectively. The mole fraction of co-assembly (f_{c}) is calculated according to the monomer–dimer equilibrium model (Eq. S4) and is given by Eq. S5.^{S2}



$$f_{\text{c}} = \frac{2[\text{M}_2]}{[\text{M}] + 2[\text{M}_2]} = \frac{\sqrt{1 + 8K_{\text{a}}[\text{M}]_0} - 1}{\sqrt{1 + 8K_{\text{a}}[\text{M}]_0} + 1} \quad \text{Eq. (S5)}$$

Where K_{a} is the observed association constant, and the zero subscript indicates total concentration. By combining Eq. S3–S5, Eq. S6 is obtained.^{S3}

$$\delta_{\text{obs}} = \delta_{\text{m}} + (\delta_{\text{c}} - \delta_{\text{m}}) f_{\text{c}} = \delta_{\text{m}} + (\delta_{\text{c}} - \delta_{\text{m}}) \times \frac{\sqrt{1 + 8K_{\text{a}}[\text{M}]_0} - 1}{\sqrt{1 + 8K_{\text{a}}[\text{M}]_0} + 1} \quad \text{Eq. (S6)}$$

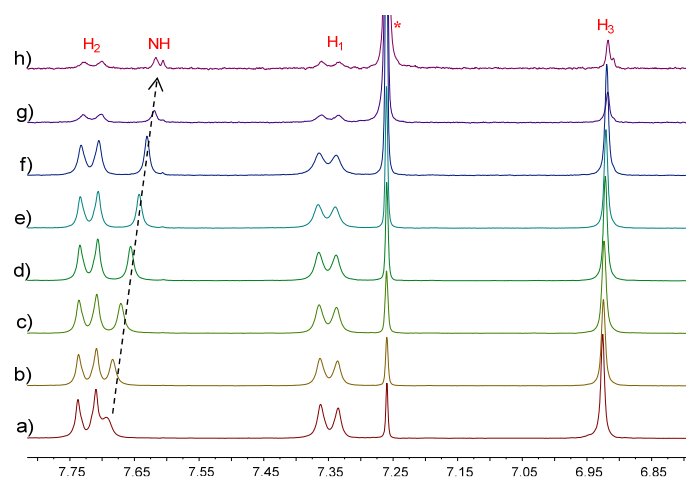


Figure S20. Partial ^1H NMR spectra (300 MHz, CDCl_3 , 298 K) of **2** upon dilution from 30.0 to 0.30 mM. The arrow shows the chemical shift changes of NH protons.

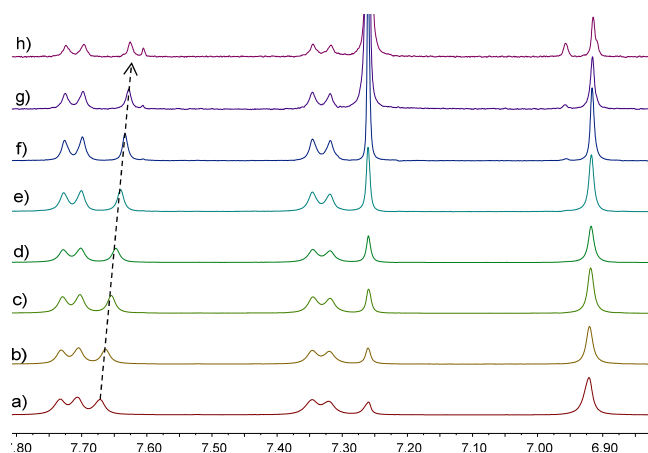


Figure S21. Partial ^1H NMR spectra (300 MHz, CDCl_3 , 298 K) of **3** upon dilution from 30.0 to 0.30 mM. The arrow shows the chemical shift changes of NH protons.

8. Fluorescent measurements of 1–3

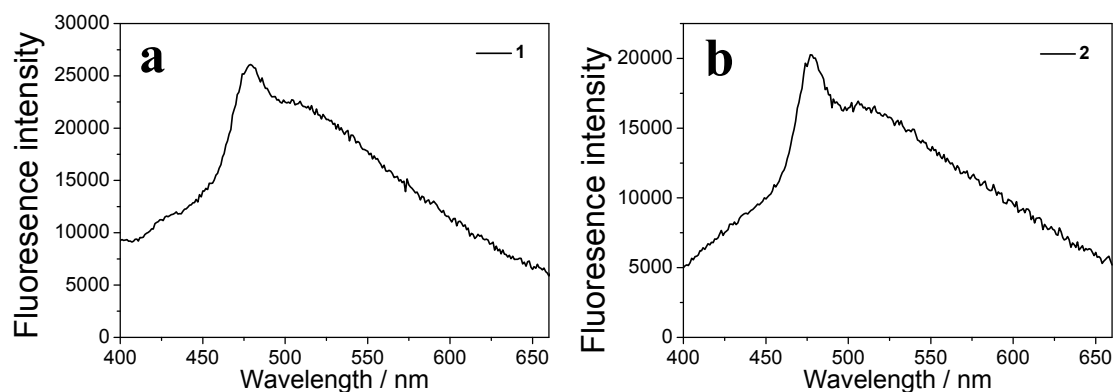


Figure S22. Emission spectra of a) **1** and b) **2** in the gel states ($\lambda_{\text{ex}} = 350$ nm). The apparent broader emission tail in the longer wavelength region should be ascribed to the scattering effect induced by gelation.^{S4}

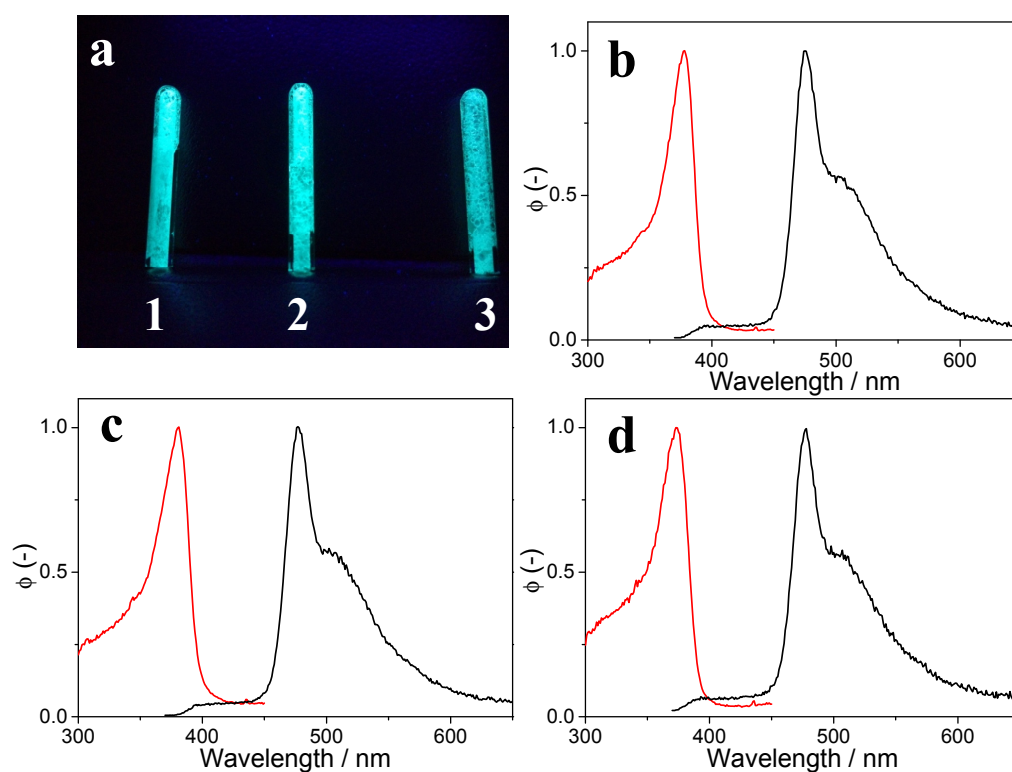


Figure S23. a) The images of doped poly(methyl methacrylate) (PMMA) films (0.5% of **1–3** in PMMA) when irradiating with 365 nm lamp. Normalized emission peak (black line, $\lambda_{\text{ex}} = 350$ nm) and excitation spectra (red line, $\lambda_{\text{em}} = 477$ nm) of b) **1**; c) **2**; and d) **3** in the film state. The reduced conformational flexibility for **1–3** in the film state suppresses the non-radiative decay process to a large extent, leading to the significant enhancement of the fluorescent signals.

References:

- S1. M. Peterca, M. R. Imam, V. Percec, *J. Am. Chem. Soc.*, **2011**, *133*, 2311–232.
- S2. J. S.Cheng, R. B. Shirts, *J. Phys. Chem.*, **1985**, *89*, 1643–1646.
- S3. A. Laederach, K. W. Cradic, K. N. Brazin, J. Zamoon, D. B. Fulton, X.-Y. Huang, A. H. Andreotti, *Protein Sci.*, **2002**, *11*, 36–45.
- S4. Y. J. Tian, E. W. Meijer, F. Wang, *Chem. Commun.*, **2013**, *49*, 9197–9199.